JOURNAL OF APPLIED ELECTROCHEMISTRY 17 (1987) 635–640

Mono- and multilayer formation studies of silver chloride on silver electrodes from chloride-containing solutions

S. JAYA, T. PRASADA RAO*, G. PRABHAKARA RAO

Central Electrochemical Research Institute, Karaikudi 623 006, India

Received 4 May 1986; revised 15 July 1986

Cyclic voltammetric and single potential step current–time transient experiments were carried out on the silver electrode in the presence of different concentrations of chloride. A monolayer peak was noticed at potentials more negative to the Ag/AgCl reversible potential. Cyclic voltammetric studies led to the conclusion that mono- and multilayer formation of silver chloride occur by adsorption–desorption (desad) and nucleation–growth processes respectively. Potentiostatic current–time transients revealed additional information, i.e. the presence of coupled nucleation–growth and desad kinetic processes during monolayer formation.

1. Introduction

The widespread use of the Ag/AgCl electrode both as a battery material and as a reference electrode has led to numerous investigations into its behaviour [1–8]. Despite the extensive literature available, there is still disagreement over the mechanism by which AgCl films nucleate and grow on an anodized silver surface [8]. Considerable evidence exists for a dissolution–precipitation mechanism whereby silver is dissolved as a polychloro complex, $AgCl_{n+1}^{n-}$ where $n = 1$, 2 or 3 according to thermodynamic stabilities of complexes [7, 8]. Recently, by analysing the current transients obtained by using a scratched silver electrode surface held under potential control it was shown that a mechanism of random oxidation of exposed metal atoms occurred [9]. Schultze *et al.* [10] reviewed the possible mechanism during anodic film formation. Similarly Angerstein-Kozlowska *et al.* [11] and Laviron [12] discussed the characteristics of linear sweep and cyclic voltammetric curves obtained during monolayer formation of strongly adsorbed, surface-bound species. This paper reports the results obtained during cyclic voltammetric and potentiostatic current–time transient experiments conducted to elucidate the mono- and multilayer formation of silver chloride. Similar studies reported earlier [13] resulted in an understanding of the nature of anodic film formation of Ag_2S on the silver electrode.

2. Experimental details

Silver electrodes (Johnson Mathey, 99.999%), in the form of mechanically polished and degreased discs of diameter 7 mm, were pressure-fitted into a Teflon holder and set in which Araldite. Deaeration was achieved by bubbling pure N_2 through the electrolyte. A Luggin probe was positioned ~ 1 mm from the electrode surface. Under these conditions the maximum deviation from the programmed potential due to electrolyte resistance was < 50 mV. The potentials were measured with respect to a normal calomel electrode (1 N). The potential of the working electrode was controlled by a Wenking potentiostat with a response time of $\sim 1\,\mu$s fed by a voltage scan generator (Model VSG 72), supplying current to a platinum counter electrode of area $\sim 6\,cm^2$.

* To whom correspondence should be addressed at: Regional Research Laboratory, Industrial Estate PO, Trivandrum 695 019, India.

0021–891X/87 $03.00 + .12

Electrolytes were made from analytical grade reagents and triply distilled water (distilled from an all-quartz triple-distillation unit). A Ricadenki xy/t recorder with a pen speed of 120 cm s^{-1} was used for recording current–potential and current–time profiles in cyclic voltammetric and potential step experiments, respectively. Experiments were conducted at 303 K.

3. Results and discussion

3.1. *Multilayer formation studies*

3.1.1. Cyclic voltammetric studies. The anodic film formation of silver chloride from quiescent solutions of 0.1 M potassium chloride in 0.1 M sodium nitrate onto a polycrystalline silver electrode was studied by subjecting the electrode to triangular scans of potential as described by Fletcher *et al.* [14] for the deposition of metals on glassy carbon, i.e. by reversing the anodic scan in the initial stages of crystallization where intercrystal collisons were absent. The main features of such a cyclic voltammogram as seen from curve B in Fig. 1 are:

(i) a rapid rise in current during the forward scan once nucleation begins,

(ii) an anodic current maximum on the reverse scan,

(iii) a characteristic cross-over loop, and

(iv) a single cathodic reduction peak corresponding to the film formed at anodic potentials.

These features indicate three-dimensional nucleation and subsequent grain growth processes. Further, on changing the sweep rate or potential limit of the triangular scan (not shown in Fig. 1), the cross-over potential remains constant. This indicates that interfacial-controlled, nucleation-growth kinetic processes are operative during multilayer formation of AgCl [14]. Such cross-over potential is indeed the Nernst reversible potential of the system for a chloride concentration of 0.1 M as described elsewhere [15]. Similar observations and conclusions were drawn when the KCl concentration was maintained at ~0.01 M or 0.001 M while retaining the ionic strength constant at 0.1 M $NaNO_3$. On the other hand, by decreasing the KCl concentrations less than 10^{-3} M, the cross-over loops were conspicuously absent, thus indicating the absence of three-dimensional nucleation–growth processes.

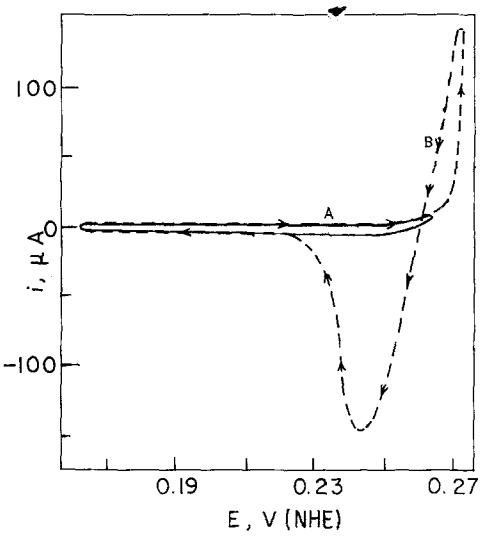

Fig. 1. Effect of varying the lower limiting potential, $E(T)$, of triangular scans during the multilayer formation of AgCl from 0.1 M KCl in 0.1 M $NaNO_3$ solution onto silver. $E(T)$ = 0.26 and 0.27 V versus NHE for curves A and B, respectively. Sweep rate, 6 mV s^{-1}.

Curve A in Fig. 2 shows the plot of the cross-over potential (which remained constant on change of sweep rate and potential limit of the triangular scan) values versus $p[Cl^-]$. Curve B shows the plot of theoretical reversible potentials [1] of the Ag/AgCl electrode versus $p[Cl^-]$ for which the thermodynamic relationship is given by Equation 1:

$$E_r \text{ (mV NHE)} = 226 - 59.1 \log [Cl^-] \quad (1)$$

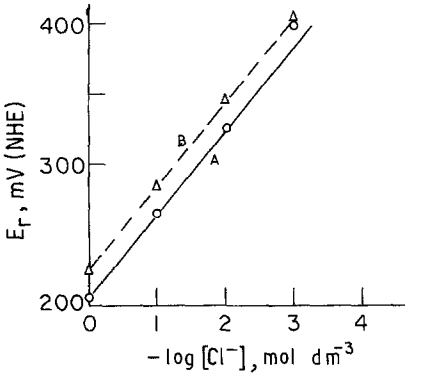

Fig. 2. Plot of Nernstian reversible potential as a function of NaCl concentration. Curve A, experimental; curve B, theoretical.

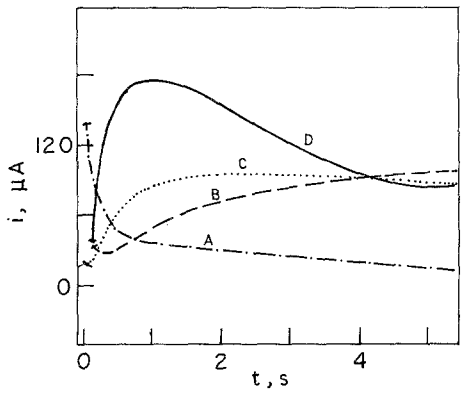

Fig. 3. Potentiostatic current–time transients for the electrode position of AgCl on silver from 0.1 M KCl in aqueous 0.1 M $NaNO_3$ solution, and at overpotentials of 45, 50, 55 and 60 mV (curves A, B, C and D, respectively).

The experimental data given in curve A of Fig. 2 can be expressed in the form of Equation 2:

$$E_r \text{ (mV NHE)} = 205 - 59 \log [Cl^-] \quad (2)$$

The agreement between the above two equations is reasonable. The fact that this measured value of E_r is a function of chloride concentration shows that it is not controlled by the onset of dissolution of Ag^+ from the silver electrode surface, since one would expect easier dissolution to occur at lower chloride concentrations [9].

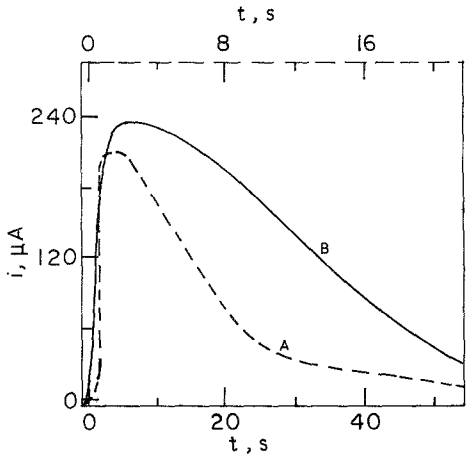

Fig. 4. Potentiostatic current–time transients obtained by holding at an overpotential of 58 (curve A) and 70 mV (curve B) respectively. Other conditions are the same as for Fig. 3.

3.1.2. Current–time transient studies. Single-step potentiostatic current–time (i–t) transients were obtained at various overpotentials and several are shown in Figs 3 and 4. The effects of nucleation are more clearly evident from the i–t transients. A significant anodic film formation occurs at overpotentials $\geqslant 50$ mV. From the nature of the i–t transients, it is clearly seen that the anodic film formation of AgCl occurs by film growth control and not by a metal dissolution control process [16]. Scharifker and Hills [17] have observed three-dimensional nucleation–growth processes, a common phenomenon in the electrodeposition of metals, during anodic film formation of Cu_2S. Such behaviour was also predicted if the deposit was a good electronic conductor. Similar criteria were checked to elucidate the nature of the kinetic processes during the multilayer formation of AgCl on silver. Thus, the principal rising part of each current transient obtained from 0.1 M KCl is a linear function of $t^{1/2}$ (cf. Fig. 5), indicating instantaneous nucleation processes. However, the current values regress to a positive intercept on the time axis and this intercept is potential-dependent (not shown in figure). Further analysis of the early stages of deposition, e.g. by means of log i–log t plots as in Fig. 6, shows that there is a transition from an i–$t^{3/2}$ to an i–$t^{1/2}$ relationship indicating that after a period of progressive nucleation, instantaneous behaviour follows with a certain time delay [18].

Non-dimensional plots of i^2/i_m^2 versus t/t_m show that the formation of AgCl on silver occurs by instantaneous nucleation processes. Further, the value of $i_m^2 t_m$ is independent of overpotential (cf. Table 1) within experimental error. From the

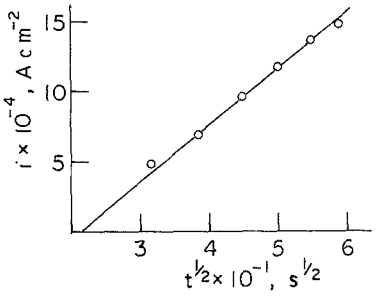

Fig. 5. Linear dependence between current and $t^{1/2}$ for the middle, rising section of transient (Fig. 3, curve D).

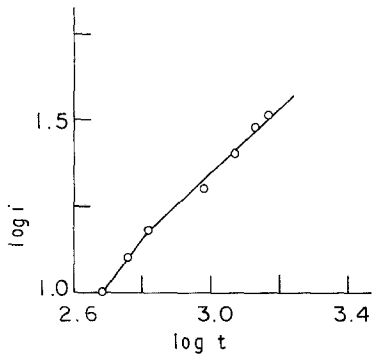

Fig. 6. Log i–log t plots of the early parts of potentiostatic transients under conditions similar to those obtained in Fig. 3.

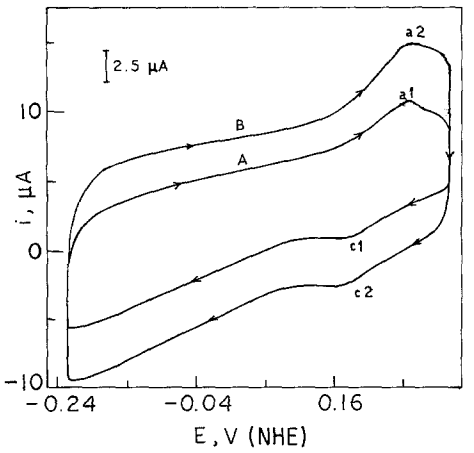

Fig. 7. Cyclic voltammograms obtained with a polycrystalline silver disc electrode in 0.01 M KCl containing 0.1 M $NaNO_3$ as supporting electrolyte in the potential scan range −0.24 to 0.32 V versus NHE. Sweep rates: 100 mV s^{-1} (curve A); 188 mV s^{-1} (curve B).

mean value of 20.09 × 10^{-6} A^2 S cm^{-4}, and the known concentration of Cl^- ions in solution, the diffusion coefficient is calculated to be 0.13 × 10^{-5} cm^2 S^{-1} from the equation $i_m^2 t_m = 0.1629 (zFc)^2 D$ [17]. This value is in good agreement with that obtained from the i versus $t^{-1/2}$ plot of the decaying portion of high overpotential transients by using the Cottrell equation.

3.2. *Monolayer formation studies*

3.2.1. Cyclic voltammetric studies. Fig. 7 shows two representative cyclic voltammograms obtained at sweep rates of 100 and 188 mV s^{-1} in the potential scan range of −0.24 to 0.32 V during electrodeposition of AgCl on silver from 0.01 M KCl in aqueous 0.1 M $NaNO_3$. It is clear that a single monolayer peak occurs at 0.25 V (peak a_1) much below the reversible potential of Ag/AgCl, namely 0.325 V. The corresponding cathodic peak (c_1) occurs at 0.18 V. The plot of peak current (i_p) (measured from the base line of the corresponding charging currents) with sweep rate (v) gives a linear plot (cf. Fig. 8) for the anodic film formation (curve A) and its subsequent reduction (curve B), which clearly indicates that the anodic peak at 0.25 V is due to the monolayer formation of AgCl. This is further confirmed by the fact that the charge associated with peak a_1 during anodic film formation in AgCl is found to be 4.62 μC cm^{-2}. It is pertinent to mention here that although the charge density associated with the anodic peak is less compared with full monolayer coverage (150 μC cm^{-2}) [9], the monolayer peaks are highly reproducible.

The monolayer peaks thus identified were subjected to analysis according to the theoretical models suggested by Bosco and Rangarajan [19] to distinguish between nucleation–growth and desad kinetic processes that are operative during monolayer formation. Thus, on changing the sweep rate from 30 to 400 mV s^{-1}, the peak width at half height ($\Delta E_{1/2}$) remains unaltered at

Table 1. Analysis of current maxima for electrodeposition of AgCl on silver

E (*mV vs NHE*)	η (*mV*)	$10^3 \times i_m$ ($A\,cm^{-2}$)	t_m (*s*)	$10^6 \times i_m^2 t_m$ ($A^2 s\,cm^{-4}$)
320	55	2.60	3.00	20.28
323	58	3.80	1.40	20.22
325	60	4.60	0.95	20.09
326	61	4.80	0.86	19.81
328	63	5.20	0.74	20.01
330	65	5.79	0.60	20.12

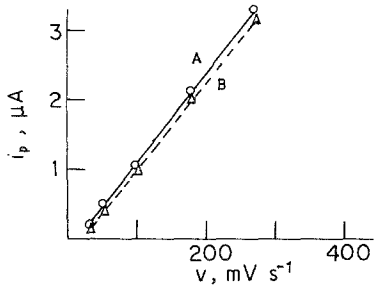

Fig. 8. Plot of peak currents of monolayer peaks of Fig. 7 (a and c) with sweep rate.

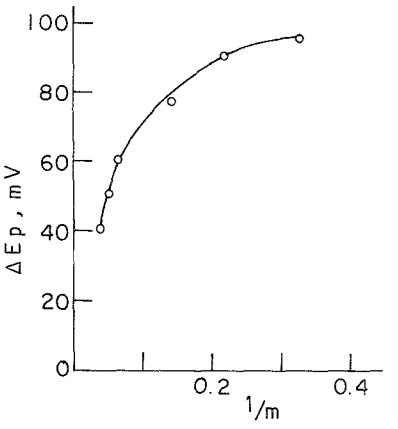

Fig. 9. Plot of ΔE_p versus $1/m$.

~ 125 mV, indicating that monolayer formation occurs by desad kinetic processes. The anodic (E_{pa}) and cathodic (E_{pc}) peak potentials of the monolayer and the difference between them (ΔE_p) at various sweep rates are listed in Table 2. The peak potentials of a and c shift in the direction of the potential scan, indicating the irreversibility of the monolayer formation of AgCl and its reduction. Further, peaks a and c are not symmetrical with respect to the potential axis in the sweep rate range investigated which confirms the irreversibility of the monolayer formation of AgCl and its subsequent reduction. Thus, from the ΔE_p value for a and c, when $V_a = V_c = 0.1\,V\,s^{-1}$, the heterogenous rate constant (k_s) value was calculated to be $32.52\,s^{-1}$. Further, the value of ΔE_p increased with increase of $1/m$ (Fig. 9) where $1/m$ is given by $RT/F(Ks/nv)$ [12]. The charge transfer coefficient (α) was calculated to be 0.5 by equating $\Delta E_{1/2}$ at higher sweep rates to $62.5/Z$ ($Z = 1$ in this case).

3.2.2. Current–time transient studies. Fig. 10 shows a few examples of *i–t* transients obtained by potentiostating the silver electrode at different potentials, namely 0.24 V (curve A) and 0.25 V (curve B) during electrodeposition of AgCl on silver. A rapidly falling current transient and a maximum–minimum at lower and higher times indicates the presence of adsorption and nucleation-growth processes respectively [16, 20]. These features clearly show that the monolayer formation of AgCl does not occur solely by adsorption as concluded in cyclic voltammetric studies. The above *i–t* transients were quantitatively analysed by the theoretical models suggested by Bosco and Rangarajan [20] for monolayer formation as they take into account the occurrence of coupled nucleation–growth and desad kinetic processes, unlike earlier models which dealt with either one of them. The contributions of different kinetic processes during monolayer formation of AgCl were determined from the parametric plots constructed as described elsewhere [13, 20]. Curve A in Fig. 11 shows that the plot of $I(e^T)$ versus

Table 2. Effect of sweep rate

Sweep rate (V mVs^{-1})	*Peak potential* (*V vs NCE*)		*Peak potential at difference* ($\Delta E_p = E_{pa} - E_{pc}$ (*mV*))
	Anodic (E_{pa})	*Cathodic* (E_{pc})	
30	0.240	0.200	40
40	0.245	0.195	50
50	0.245	0.190	55
100	0.250	0.180	70
180	0.260	0.170	90
270	0.265	0.170	95
400	0.270	–	–

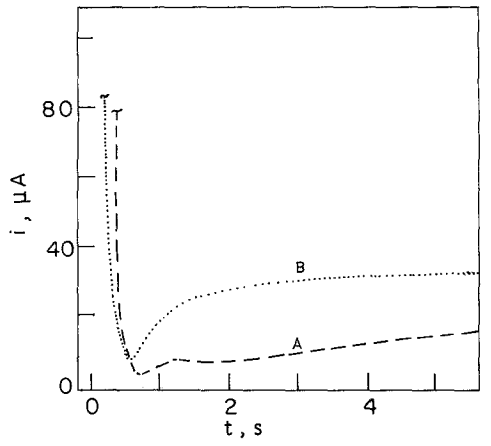

Fig. 10. Potentiostatic current–time transients during monolayer formation of AgCl from 0.01 M KCl in aqueous 0.1 M $NaNO_3$ by stepping the potential from 0.12 V to 0.24 V (curve A) and 0.25 V (curve B).

$T(e^T)$ (where I and T are non-dimensional current and time, respectively), is linear with an intercept indicating that the nucleation–growth processes are instantaneous in nature (not progressive as when $I(e^T)$ versus $T^2(e^T)$ is non-linear, cf. curve B, Fig. 11). The I and T are related to current and time as defined below.

$$I = i/\nu_m$$

$$T = \mu t$$

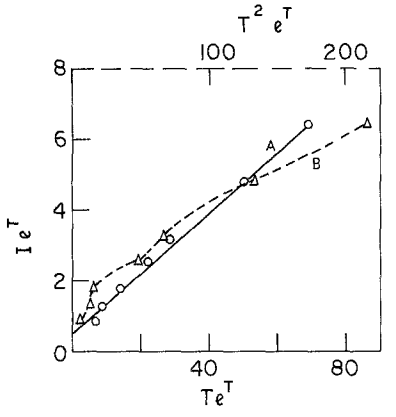

Fig. 11. Plot of Ie^T versus Te^T (curve A) or T^2e^T (curve B) for the current–time transient of Fig. 9, curve B. I and T are non-dimensional quantities.

where ν_m is the monolayer charge, and

$$\mu = \vec{k} + \overleftarrow{k}$$

where $\vec{k}$ is the adsorption rate constant and $\overleftarrow{k}$ is the desorption rate constant.

The adsorption (G) and instantaneous nucleation–growth (D_1) constants (non-dimensional) were calculated to be 0.5 and 0.042 from the intercept and slope values, respectively. In conclusion, the monolayer formation of AgCl occurs mainly by adsorption–desorption processes with a minor contribution from instantaneous nucleation–growth controlled processes.

References

[1] D. J. G. Ives and G. J. Janz, 'Reference Electrodes', Academic Press, New York (1961) pp. 54, 184.
[2] H. Lal, H. R. Thirsk and W. F. K. Wynne-Jones, *Trans. Faraday Soc.* **47** (1951) 70.
[3] H. R. Thirsk and W. F. K. Wynne-Jones, *ibid.* **47** (1951) 999.
[4] W. Jaenicke, R. P. Tischer and H. Gerischer, *Z. Electrochem.* **59** (1955) 448.
[5] M. Fleischmann and H. R. Thirsk, *Electrochim. Acta* **1** (1959) 146.
[6] T. Katan, S. Szpak and D. M. Bennion, *J. Electrochem. Soc.* **121** (1974) 757.
[7] R. D. Giles, *J. Electroanal. Chem.* **27** (1970) 11.
[8] T. Katan, S. Szpak and D. M. Bennion, *J. Electrochem. Soc.* **120** (1973) 883.
[9] G. T. Burstein and R. D. K. Misra, *Electrochim. Acta* **28** (1983) 363, 370.
[10] J. W. Schultze, M. M. Lohrengel and D. Ross, *ibid.* **28** (1983) 973.
[11] H. Angerstein-Kozlowska, J. Klinger and B. E. Conway, *J. Electroanal Chem.* **75** (1977) 45.
[12] E. Laviron, *ibid.* **101** (1979) 19.
[13] S. Jaya, T. P. Rao and G. P. Rao, *Bull. Electrochem.* **2** (1986) 313.
[14] S. Fletcher, C. S. Halliday, D. Gates, M. Westcott, T. Lwin and G. Nelson, *J. Electroanal. Chem.* **159** (1983) 267.
[15] S. Fletcher, *Electrochim. Acta* **28** (1983) 917.
[16] D. A. Varmilyea in 'Advances in Electrochemistry and Electrochemical Engineering', Vol. 3 (edited by P. Delahay), Interscience, New York (1971).
[17] B. Scharifker and G. J. Hills, *Electrochim. Acta* **28** (1983) 879.
[18] G. A. Gunawardena, G. J. Hills, I. Montenegro and B. R. Scharifker, *J. Electroanal. Chem.* **138** (1982) 225.
[19] E. Bosco and S. K. Rangarajan, *ibid.* **129** (1981) 25.
[20] *Idem, J. Chem. Soc., Faraday Trans. I* **77** (1981) 1673.